Virtual actuators with virtual sensors

P J Gawthrop
Centre for Systems and Control, Department of Mechanical Engineering, University of Glasgow, James Watt Building, Glasgow G12 8QQ, UK. email: P.Gawthrop@eng.gla.ac.uk

The manuscript was received on 21 December 2004 and was accepted after revision for publication on 27 April 2005.

DOI: 10.1243/095965105X33473

Abstract: The virtual actuator approach to bond graph based control is extended to use virtual sensor inputs; this allows relative degree conditions on the controller to be relaxed. Furthermore, the effect of the transfer system can be eliminated from the closed-loop system. Illustrative examples are given.

Keywords: bond graphs, control systems, virtual actuators, virtual sensors, substructuring

1 INTRODUCTION

The virtual actuator [**1**] approach to bond graph based control was introduced by Gawthrop *et al.* [**2**], applied to an experimental ball and beam system by Gawthrop [**1**] and to an inverted pendulum by Gawthrop and Ballance [**3**]. The approach has the advantage that the physical controller can be designed as if a collocated source/sensor pair were available. Moreover, it has been shown by Gawthrop *et al.* [**4**] that the same approach can be applied to real-time numerical–experimental substructure-based testing of structures under dynamic loading [**5**, **6**].

This technical note extends the results of reference [**1**] in two ways: the first relative degree constraint ($\sigma_y \geqslant \sigma$) presented in Design rule 1 of reference [**1**] is ameliorated and, optionally, the transfer system is eliminated from the closed-loop system. This technical note is based on, and must be read in conjunction with, reference [**1**]; the discussion is restricted to linear, time-invariant single-input single-output systems. In parallel with the bond graph development, a transfer function/relative degree interpretation is provided to improve accessibility to those not expert in bond graph methods and the concept of shortest causal path. The power of the methods discussed in this paper can best be realized using symbolic algebra-based bond graph tools such as model transformation tools (MTT) [**7**] (http://mtt.sf.net). To obtain readable transfer functions, however, symbols are sometimes replaced by numbers in the examples.

The outline of the paper is as follows. Section 2 summarizes the results of reference [**1**] and discusses the limitations using a simple example. Section 3 introduces virtual sensors in this context and illustrates the advantages of the new approach using examples. Section 4 concludes the paper and suggests future research directions.

2 VIRTUAL ACTUATORS

Figure 1(a) is an abstract version of Fig. 5(a) in reference [**1**] and shows the basic ideas of virtual actuator control. For simplicity, it is assumed that the measured output y_s is an effort and the input u is a flow. Obvious changes can be made if this is not the case.

Reference [**1**] decomposes the controlled system into two subsystems with the rather unhelpful names 'sub$_1$' and 'sub$_2$'. Following reference [**4**], this paper uses the name 'transfer system' in place of 'sub$_1$' to denote that part of the system between the system input u and the junction to which the virtual junction is to be attached; this is denoted **Tra** in Fig. 1(a). The subsystem called 'sub$_2$' in Fig. 5(a) in reference [**1**], representing that part of the system to be explicitly controlled, is now called **Sys** in Fig. 1(a).

In terms of this paper, Assumption 1 in reference [**1**] can be rephrased as follows.

Assumption 1

Tra and **Sys** have the transfer function representations

$$y_t = T(s)u + T_y(s)y_s \tag{1}$$

$$y_s = S(s)u_s \tag{2}$$

$$u_s = y_t \tag{3}$$

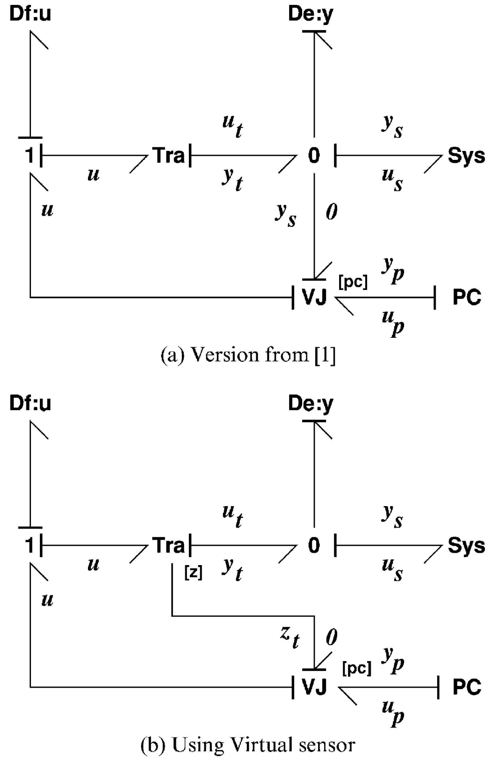

(a) Version from [1]

(b) Using Virtual sensor

Fig. 1 Virtual actuator control

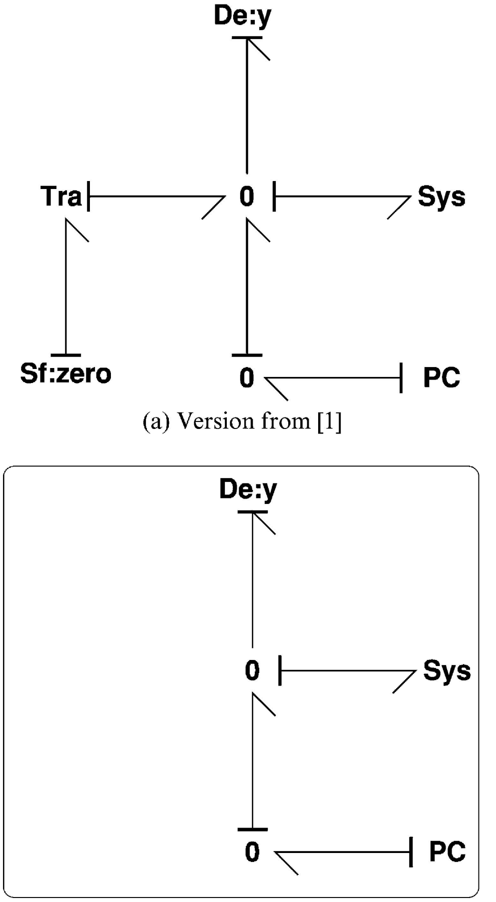

(a) Version from [1]

(b) Transfer system removed

Fig. 2 Desired closed-loop system

As in reference [**1**], **PC** represents the bond graph of the physical controller with the transfer function representation

$$u_p = C_w(s)w - C_y(s)y_p \tag{4}$$

The virtual junction component **VJ** is represented by a bicausal bond graph in the Appendix of reference [**1**] and has the transfer function representation

$$\begin{pmatrix} y_p \\ u \end{pmatrix} = V(s)\begin{pmatrix} u_p \\ y_s \end{pmatrix} \tag{5}$$

In the version presented in reference [**1**]

$$V(s) = \begin{pmatrix} 0 & 1 \\ T(s)^{-1} & 0 \end{pmatrix} \tag{6}$$

where $T(s)$ is the transfer function of the transfer system **Tra** relating u to y_t.

Combining equations (5) and (4) gives the controller explicitly as

$$u = T(s)^{-1}C_w(s)w + T(s)^{-1}C_y(s)y_p \tag{7}$$

This controller leads to a closed-loop system equivalent to that of Fig. 2(a).

As discussed previously in Design rule 1 of reference [**1**], the requirement that the two transfer functions in equation (7) be proper leads to the conclusion that the relative degree σ of $T(s)$, the relative degree σ_w of $C_w(s)$ and the relative degree σ_y of $C_y(s)$ are related by

$$\sigma_y \geqslant \sigma \tag{8}$$

$$\sigma_w \geqslant \sigma \tag{9}$$

A shortest causal path (SCP) [**8**] interpretation is given in reference [**1**].

2.1 Example: two coupled tanks

This example is discussed in section 3.3 in reference [**1**]. In the notation of this paper

$$T(s) = \frac{1}{1 + r_1 c_1 s} \tag{10}$$

$$T_y(s) = \frac{-c_1 s}{1 + r_1 c_1 s} \tag{11}$$

$$C_y(s) = C_w(s) = \frac{1}{r_c + i_c s} \tag{12}$$

If $i_c \neq 0$, $\sigma_y = \sigma_w = \sigma = 1$, thus satisfying equations (8) and (9). However, if $i_c = 0$, then $\sigma_y = \sigma_w = 0$ and both equations (8) and (9) are violated.

The virtual junction equation (6) becomes

$$V(s) = \begin{pmatrix} 0 & 1 \\ 1 + r_1 c_1 s & 0 \end{pmatrix} \tag{13}$$

The controller equation (14) becomes

$$u = \frac{1 + r_1 c_1 s}{r_c + i_c s}(w - y_p) \tag{14}$$

As predicted by equations (8) and (9), the controller equation (14) is proper as long as $i_c \neq 0$; however, if $i_c = 0$ it is improper. The closed-loop system corresponding to Fig. 1(a) is given in equation (8) of reference [**1**] as

$$y_s = \frac{s+1}{(s^2 + 3s + 1)(r_c + i_c s) + s + 1} w \tag{15}$$

where the substitutions $r_1 = c_1 = r_2 = c_2 = 1$ have been made for clarity. Equation (14) also corresponds to the desired closed-loop sytem of Fig. 2(a). The problem arising when $i_c = 0$ is solved in section 3.

2.2 Removing the transfer system

As discussed by Gawthrop *et al.* [**4**], it is sometimes of interest to remove the effect of **Tra** from the desired closed-loop system of Fig. 2(a) to give that of Fig. 2(b). In view of equation (1), this can be achieved by replacing $V(s)$ in equation (5) by

$$V(s) = \begin{pmatrix} 0 & 1 \\ T(s)^{-1} & -T(s)^{-1}T_y(s) \end{pmatrix} \tag{16}$$

thus replacing equation (7) by

$$u = T(s)^{-1}C_w(s)w + T(s)^{-1}[C_y(s) - T_y(s)]y_p \tag{17}$$

The term $T(s)^{-1}T_y(s)$ must also be proper. In view of equations (10) and (11), this is not the case for the example of section 2.1.

The virtual junction, represented in transfer function form by equations (5) and (16), corresponds to system inversion. As discussed in references [**9–12**] and the Appendix in reference [**1**], such inversion can be accomplished using the bicausal bond graph of Fig. 3(a).

2.3 Example: two coupled tanks (continued)

The transfer function $T(s)$ of equation (1) is given by equation (10) and $T_y(s)$ is given by equation (11). It follows from equation (16) that

$$V(s) = \begin{pmatrix} 0 & 1 \\ (1 + r_1 c_1 s) & c_1 s \end{pmatrix} \tag{18}$$

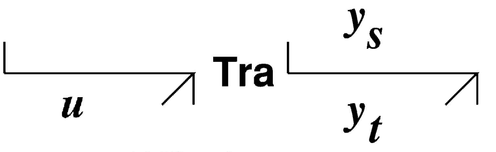

(a) Virtual actuator

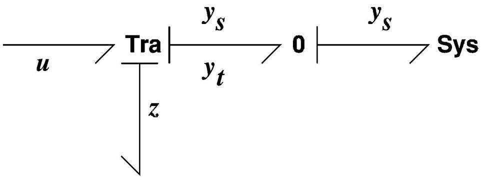

(b) Virtual sensor

Fig. 3 System inversion

Thus the controller equation (17) contains the term $c_1 s y_p$, which cannot be implemented.

Section 3 shows how this particular problem can be overcome in general.

3 VIRTUAL SENSORS

In essence, the virtual actuator approach of Fig. 1(a) moves the actuation signal u_p from the physical controller **PC** to the input of the transfer system **Tra** using the **VJ** component. In this section, the measurement signal y_p acting on **PC** is also moved to another output z of **Tra** again using an extended **VJ** component as in Fig. 1(b). Thus the virtual actuator approach is combined with a virtual sensor approach.

However, the following assumption is required.

Assumption 2

The transfer system output y_t can be expressed in terms of the auxiliary measurement z as

$$y_t = \tilde{T}(s)z + \tilde{T}_y(s)y_s \tag{19}$$

Note that Assumption 2 implies that y_t can be expressed in terms of z without explicit dependency on u. If Assumption 2 is correct, it follows from equations (19) and (1) to (3) that the measured signal y_p imposed on **PC** can be expressed in terms of z (only) as

$$y_p = y_s = Z(s)z \tag{20}$$

$$Z(s) = [1 - \tilde{T}_y(s)S(s)]^{-1}S(s)\tilde{T}(s)z \tag{21}$$

The partial inversion implied by equation (21) has the bond graph interpretation of Fig. 3(b).

The virtual junction equations (5), (6), and (16) can then be replaced by

$$\begin{pmatrix} y_p \\ u \end{pmatrix} = V_z(s) \begin{pmatrix} u_p \\ z \end{pmatrix} \tag{22}$$

and

$$V_z(s) = \begin{cases} \begin{pmatrix} 0 & Z(s) \\ T(s)^{-1} & 0 \end{pmatrix} & \text{if } \mathbf{Tra} \text{ is to remain} \\ \begin{pmatrix} 0 & Z(s) \\ T(s)^{-1} & -T(s)^{-1}T_y(s)Z(s) \end{pmatrix} & \text{if } \mathbf{Tra} \text{ is to be removed} \end{cases} \tag{23}$$

The corresponding controller is

$$\begin{aligned} u &= T(s)^{-1}C_w(s)w \\ &\quad + (T(s)^{-1}C_y(s) - T(s)^{-1}T_y(s))Z(s)z \end{aligned} \tag{24}$$

Comparing equations (17) and (24) reveals that y_s is replaced by $Z(s)z$.

The transfer function $T(s)^{-1}T_y(s)Z(s)$ must be proper. This is a property of the system, not the controller, and so is expressed as follows.

Assumption 3

Let σ, σ', and σ_z be the relative degrees of the transfer functions $T(s)$, $T_y(s)$, and $Z(s)$ respectively. Then

$$\sigma' \geqslant \sigma - \sigma_z \tag{25}$$

Similarly, the transfer functions $T(s)^{-1}C_y(s)Z(s)$ and $T(s)^{-1}C_w(s)Z(s)$ must also be proper. These transfer functions are dependent on the transfer functions $C_y(s)$ and $C_w(s)$ of the (user-chosen) physical controller **PC**. It follows that Design rule 1 in reference [**1**] is replaced by the following.

Design rule 1

The relative degrees σ and σ_z are defined in Assumption 3. Let σ_y and σ_w be the relative degrees of the transfer functions $C_y(s)$ and $C_w(s)$ respectively. Then

$$\sigma_y \geqslant \sigma - \sigma_z \tag{26}$$

$$\sigma_w \geqslant \sigma \tag{27}$$

Inequality (26) differs from that of Design rule 1 in reference [**1**] due to the presence of the term σ_z and is therefore more readily satisfied, whereas inequality (27) is the same as before. However, inequality (27) is readily satisfied by filtering the setpoint w by a low-pass filter of sufficient relative degree.

3.1 Example: two coupled tanks (continued)

Choosing z to be the pressure in the first coupled tank of Fig. 4 in reference [**1**], that is the effort associated with **C:c_1** of Fig. 5(a) in reference [**1**], gives

$$\tilde{T} = \frac{1}{r_1} = -\tilde{T}_y \tag{28}$$

$$S(s) = \frac{r_2}{1 + r_2 c_2 s} \tag{29}$$

$$Z(s) = \frac{r_2}{(r_1 + r_2) + r_1 r_2 c_2 s} \tag{30}$$

Therefore $\sigma_z = 1$ and, from equations (10) and (11), $\sigma = 1$ and $\sigma' = 0$. From Design rule 1, it is required that $\sigma_y \geqslant 0$ and $\sigma_w \geqslant 1$. The former is weaker than the equivalent condition in Example 2.1, but the latter is the same. From equation (12)

$$\sigma_y = \sigma_w = \begin{cases} 0 & \text{if } i_c = 0 \\ 1 & \text{if } i_c \neq 0 \end{cases} \tag{31}$$

However, as mentioned previously, a first-order low-pass filter could be used to increase the relative degree of $C_w(s)$. The virtual junction equations are

$$V_z(s) = \begin{cases} \begin{pmatrix} 0 & \dfrac{1}{s+2} \\ (1+s) & 0 \end{pmatrix} & \text{if } \mathbf{Tra} \text{ is to remain} \\ \begin{pmatrix} 0 & \dfrac{1}{s+2} \\ (1+s) & \dfrac{s}{s+2} \end{pmatrix} & \text{if } \mathbf{Tra} \text{ is to be removed} \end{cases} \tag{32}$$

where the substitutions $r_1 = c_1 = r_2 = c_2 = 1$ have been made for clarity. The corresponding controller is given by

$$u = \frac{s+1}{i_c s + r_c} w - \frac{(i_c s + r_c)s - (s+1)}{(i_c s + r_c)(s+2)} z \tag{33}$$

The relative degrees of the transfer functions in equation (33) are as predicted by equation (31).

The closed-loop system corresponding to Fig. 1(b) is

$$y_s = \frac{1}{1 + (i_c s + r_c)(s+1)} w \tag{34}$$

Unlike equation (15), equation (34) does not contain the effect of **Tra** but corresponds to the desired system of Fig. 2(b).

3.2 Example: mass–spring–damper system

Figure 4 illustrates a simple mass–spring–damper system similar to that previously used as a substructuring example (section 4 in reference [**4**]). Figure 2(b) gives the desired closed-loop system where **Sys** and **PC** are as shown in Figs 4(c) and (d); **Sys** comprises a single copy of the mass–spring–damper system of Fig. 4(a) (with the addition of the measurement z of the spring force) and **PC** comprises two copies of the mass–spring–damper system of Fig. 4(a). In the context of substructuring [**4**], **Sys** represents a physical test substructure and **PC** a numerical simulation of the remainder of the structure. Following reference [**4**], the servomechanism driving the test substructure (**Tra**) is represented by the bond graph of Fig. 4(b).

In this example, the parameters are chosen as $c_s = r_s = m_s = c_{p1} = r_{p1} = m_{p1} = c_{p2} = r_{p2} = m_{p2} = 1$, $c_t = r_t = 5$, and $m_t = 2$. This gives

$$T(s) = \frac{1}{10s^2 + 25s + 1} \tag{35}$$

$$T_y(s) = \frac{-5s}{10s^2 + 25s + 1} \tag{36}$$

$$Z(s) = \frac{s+1}{2s^3 + 7s^2 + 8s + 6} \tag{37}$$

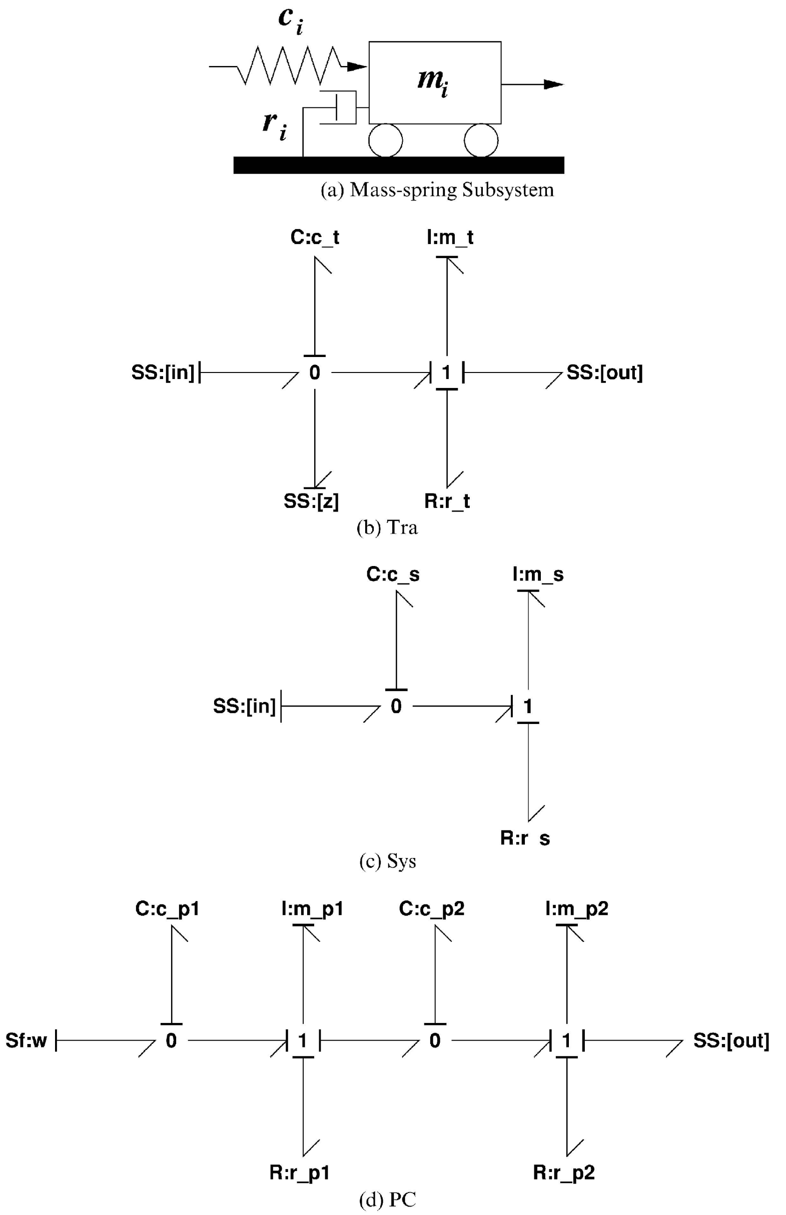

Fig. 4 Mass–spring–damper substructuring

$$C_y(s) = \frac{s(s^2+s+2)}{s^4+2s^3+4s^2+3s+1} \tag{38}$$

$$C_w(s) = \frac{1}{s^4+2s^3+4s^2+3s+1} \tag{39}$$

giving the virtual junction equations

$$V_z(s) = \begin{pmatrix} 0 & \frac{s+1}{2s^3+7s^2+8s+6} \\ (10s^2+25s+1) & \frac{5s(s+1)}{2s^3+7s^2+8s+6} \end{pmatrix} \tag{40}$$

From equations (36) to (39), $\sigma = \sigma_z = 2$, $\sigma' = \sigma_y = 1$, and $\sigma_w = 4$. Thus both Assumption 3 and Design rule 1 are satisfied and so the controller is proper. However, conditions (8) and (9), corresponding to the virtual actuator controller without the virtual sensor, are violated.

The closed-loop system corresponding to Fig. 1(b) is

$$y(s) = \frac{s+1}{s^6+3s^5+8s^4+11s^3+11s^2+6s+1} w(s) \tag{41}$$

which also corresponds to the desired system of Fig. 2(b). This is a sixth-order system corresponding to the combination of the second-order **Sys** and the fourth-order **PC**.

4 CONCLUSION

The virtual actuator method has been extended to use additional measurements to ameliorate the relative degree constraints reported in reference [**1**]. In particular, Design rule 1 in reference [**1**] is replaced by Design rule 1 here. The method is also extended to remove transfer system dynamics; this requires Assumption 3. Although expressed in terms of relative degree, these results also have the shortest causal path interpretation discussed in reference [**1**].

If z is not directly available, it could be deduced using a state observer [**13**]; this would have the advantage of explicitly including the measurement y_s in the controller. Future work will examine this possibility using the bond graph interpretation of observers given by Karnopp [**14**] and Gawthrop [**15**].

Because the feedback controllers designed using the virtual actuator approach are based on system models, the issue of the sensitivity of the resultant closed-loop system to modelling errors arises. Again, this is an important topic for future research.

Links between the virtual actuator approach and backstepping [**16**] were noted in reference [**1**], but Vink [**17**] has shown that the virtual actuator version of reference [**1**] does not correspond to backstepping in general. It is believed that combining the virtual actuator approach with the virtual sensor approach of this paper does lead to a closer match with backstepping, but this has yet to be shown.

ACKNOWLEDGEMENTS

The author is grateful to Dustin Vink and Donald Ballance for discussions on bond graphs and backstepping from which the ideas reported here arose. He would also like to thank David Wagg, Simon Neild, and Max Wallace of Bristol University for introducing him to substructuring and the anonymous referees for helpful comments on the paper.

REFERENCES

1 **Gawthrop, P. J.** Bond graph based control using virtual actuators, *Proc. Instn Mech. Engrs, Part I: J. Systems and Control Engineering*, 2004, **218**(I4), 251–268. DOI: 10.1243/0959651041165864.
2 **Gawthrop, P. J., Ballance, D. J.,** and **Vink, D.** Bond graph based control with virtual actuators. In Proceedings of the 13th European Simulation Symposium on *Simulation in Industry* (Eds N. Giambiasi and C. Frydman), Marseille, France, October 2001, pp. 813–817, SCS; ISBN 90-77039-02-3.
3 **Gawthrop, P. J.** and **Ballance, D. J.** Virtual actuator control of mechanical systems. In Proceedings of the International Conference on *Bond Graph Modeling and Simulation* (*ICBGM'05*), Simulation Series, New Orleans, Louisiana, January 2005, pp. 233–238 (Society for Computer Simulation, San Diego, USA).
4 **Gawthrop, P. J., Wallace, M. I.,** and **Wagg, D. J.** Bond-graph based substructuring of dynamical systems, *Earthquake Engng Struct. Dynamics*, 2005, **34**(6), pp. 687–703.
5 **Wagg, D. J.** and **Stoten, D. P.** Substructuring of dynamical systems via the adaptive minimal control approach, *Earthquake Engng Struct. Dynamics*, June 2001, **30**(6), 865–877.
6 **Darby, A. P., Blakeborough, A.,** and **Williams, M. S.** Improved control algorithm for real-time substructure testing, *Earthquake Engng Struct. Dynamics*, March 2001, **30**(3), 431–448.
7 **Ballance, D. J., Bevan, G. P., Gawthrop, P. J.,** and **Diston, D. J.** Model transformation tools (MTT): the open source bond graph project. In Proceedings of the International Conference on *Bond Graph Modeling and Simulation* (*ICBGM'05*), Simulation Series, New Orleans, Louisiana, January 2005, pp. 123–128 (Society for Computer Simulation, San Diego, USA).

8 **Ngwompo, R. F., Scavarda, S.,** and **Thomasset, D.** Physical model-based inversion in control systems design using bond graph representation. Part 1: theory, *Proc. Instn Mech. Engrs, Part I: J. Systems and Control Engineering*, 2001, **215**(I2), 95–103.
9 **Gawthrop, P. J.** Physical interpretation of inverse dynamics using bicausal bond graphs, *J. Franklin Inst.*, 2000, **337**(6), 743–769. DOI: 10.1016/S0016–0032(00)00051–X.
10 **Ngwompo, R. F.** and **Gawthrop, P. J.** Bond graph based simulation of nonlinear inverse systems using physical performance specifications, *J. Franklin Inst.*, November 1999, **336**(8), 1225–1247. DOI: 10.1016/S0016–0032(99)00032–0.
11 **Gawthrop, P. J.** Control system configuration: inversion and bicausal bond graphs. In Proceedings of the 1997 International Conference on *Bond Graph Modeling and Simulation* (*ICBGM'97*) (Eds J. J. Granda and G. Dauphin-Tanguy), vol. 29, Simulation Series, Phoenix, Arizona, January 1997, pp. 97–102 (Society for Computer Simulation, San Diego, USA).
12 **Gawthrop, P. J.** Bicausal bond graphs. In Proceedings of the International Conference on *Bond Graph Modeling and Simulation* (*ICBGM'95*) (Eds F. E. Cellier and J. J. Granda), vol. 27, Simulation Series, Las Vegas, Nevada, January 1995, pp. 83–88 (Society for Computer Simulation, San Diego, USA); ISBN 1-56555-037-4.
13 **Kwakernaak, H.** and **Sivan, R.** *Linear Optimal Control Systems*, 1972 (John Wiley, New York).
14 **Karnopp, D. C.** Bond graphs in control: physical state variables and observers, *J. Franklin Inst.*, 1979, **308**(3), 221–234.
15 **Gawthrop, P. J.** Physical model-based control: a bond graph approach, *J. Franklin Inst.*, 1995, **332B**(3), 285–305.
16 **Krstic, M., Kanellakopoulos, I.,** and **Kokotovic, P. V.** *Nonlinear and Adaptive Control Design*, 1995 (John Wiley, New York).
17 **Vink, D.** Aspects of bond graph modelling in control, PhD Thesis, Department of Mechanical Engineering, University of Glasgow, 2005 (submitted).

APPENDIX

Notation

$C_y(s)$, $C_w(s)$	physical controller (**PC**) transfer functions
$T(s)$	input transfer function of transfer system
$T_y(s)$	output transfer function of transfer system
$\tilde{T}(s)$	transfer function of transfer system with virtual sensor input
$\tilde{T}_y(s)$	output transfer function of transfer system with virtual sensor
u	system input (control signal)
u_p	control signal from physical controller **PC**
u_s	input to **Sys**
w	controller set-point
y_p	measurement signal at physical controller **PC**
y_t, y_s	transfer system **Tra** and system **Sys** outputs
z	measurement signal for virtual sensor
$Z(s)$	transfer function from z to y_s
σ, σ', and σ_z	relative degrees of $T(s)$, $T_y(s)$, and $Z(s)$
σ_y and σ_w	relative degrees of $C_y(s)$ and $C_w(s)$

Principle bond graph components

C:c	bond graph **C** component with parameter c
De	bond graph effort detector component
I:j	bond graph **I** component with parameter j
PC	physical controller
R:r	bond graph **R** component with parameter r
Se	bond graph effort source component
SS	bond graph source-sensor component
SS:[port], [port]	subsystem port and port label
Sys	controlled system
Tra	transfer system
VJ	virtual junction component